INSTITUTE OF PHYSICS PUBLISHING MODELLING AND SIMULATION IN MATERIALS SCIENCE AND ENGINEERING

Modelling Simul. Mater. Sci. Eng. **10** (2002) 227–236 PII: S0965-0393(02)33161-9

On the Monte Carlo simulation of curvature-driven growth

B Radhakrishnan and T Zacharia

Computer Science and Mathematics Division, Oak Ridge National Laboratory, Oak Ridge, TN 37831-6359, USA

Received 27 September 2001
Published 13 February 2002
Online at stacks.iop.org/MSMSE/10/227

Abstract
The kinetics of shrinking of an island grain embedded in a matrix as a function of the grain boundary properties is simulated using a Monte Carlo (MC) technique where the probability of switching of a grain boundary site is scaled according to the product of the boundary energy and mobility. Careful investigation of the simulation results shows that the correct implementation is one where the MC simulation time, the time of visit to a grain boundary site during the simulation is scaled according to the product of the boundary energy and mobility. Simulations in which the site is visited all the time, but the flip probability is scaled according to the product of the boundary energy and mobility, do not yield the correct results expected for curvature-driven boundary migration. The mechanistic differences between the two approaches are described.

1. Introduction

Monte Carlo (MC) simulation of curvature-driven growth was introduced in the early 1980s by the Exxon group [1]. Simulation of the shrinking of a circular grain embedded in a matrix grain of a different orientation yielded a linear relationship between the area of the circular grain vs simulation time, thus verifying the parabolic growth law. Shrinking circle simulations have also been used to establish such a relationship for curvature-driven growth using phase field [2] method. More recently, a circular half-loop geometry has been used to verify curvature-driven growth using molecular dynamics simulations [3]. For the curvature-driven shrinking of a circular island grain, the rate of change of grain area, $\mathrm{d}A/\mathrm{d}t$, varies linearly with time with a slope proportional to $\mu\gamma$, where μ is the relative boundary mobility and γ is the relative boundary energy [4]. Therefore, for the shrinking of two circular grains of mobilities μ_1 and μ_2 and energies γ_1 and γ_2, the relative value of the slopes, $(\mathrm{d}A_1/\mathrm{d}t)/(\mathrm{d}A_2/\mathrm{d}t)$ should be $\mu_1\gamma_1/\mu_2\gamma_2$. Although such a relationship has been indirectly verified for phase field and molecular dynamics simulations of curvature-driven growth [3, 5], it has not been reported in the literature for MC simulations.

In the case of curvature-driven grain growth, the total energy of the simulation domain consisting of n lattice sites is given by [1]

$$H = \sum_{i}^{n} \sum_{j}^{\mathrm{nn}} \gamma(S_i, S_j,)(1 - \delta_{S_i S_j}), \tag{1}$$

where the inner summation is taken over the nearest neighbours (nn) of a site and the outer summation is taken over all the n sites in the lattice, S_i and S_j are the orientations of the ith and jth sites that determine the magnitude γ, and δ is the Kronecker delta. The MC method involves visiting each lattice site in a random fashion and flipping the site to a randomly chosen new orientation based on the change in the local energy of the site and its neighbourhood due to the flip. Recently, Rollett and Holm [6] proposed the following probability, p, for the switching of a boundary site:

$$p(S_i, S_j, \Delta E, T) = \begin{cases} \dfrac{\gamma(S_i, S_j)\mu(S_i, S_j)}{\gamma_{\max}\mu_{\max}}, & \Delta E \leqslant 0, \\ \dfrac{\gamma(S_i, S_j)\mu(S_i, S_j)}{\gamma_{\max}\mu_{\max}} \exp\left(\dfrac{-\Delta E}{kT}\right), & \Delta E > 0, \end{cases} \tag{2}$$

where $\mu_{\max}$ and $\gamma_{\max}$ are the maximum values of the boundary mobility and energy, respectively, in the simulation domain, ΔE is the change in energy of the site and the neighbourhood as a result of the flip, k is Boltzmann constant and T is the lattice temperature. The simulation time is measured in units of Monte Carlo steps (MCS), which corresponds to one flip attempt per site for all the n sites in the simulation domain. Each MCS corresponds to a physical evolution time, which depends on the physical temperature and the jump frequency of the atoms. The flipping probability defined by equation (2) was proposed in order to simulate curvature-driven growth in domains that contain a range of boundary energies and mobilities. In [6], equation (2) is stated without proof. However, a physical reasoning for equation (2) could be provided as follows. Consider the case of a shrinking island grain. The flipping of a grain boundary site represents a change in the grain area, $\mathrm{d}A/\mathrm{d}t$, which is proportional to $\mu\gamma$, as stated previously for curvature-driven growth. Therefore, if the flip of a site adjacent to a boundary with $\mu = \mu_{\max}$ and $\gamma = \gamma_{\max}$ occurs with a probability of 1.0, then for the same interval of time the flip probability of a site adjacent to a boundary with $\mu\gamma < \mu_{\max}\gamma_{\max}$ should be given by $\mu\gamma/\mu_{\max}\gamma_{\max}$.

For zero lattice temperature simulations, equation (2) yields the following flipping probability:

$$p(S_i, S_j, \Delta E) = \begin{cases} \dfrac{\gamma(S_i, S_j)\mu(S_i, S_j)}{\gamma_{\max}\mu_{\max}}, & \Delta E \leqslant 0, \\ 0, & \Delta E > 0. \end{cases} \tag{3}$$

In this paper, we will focus on zero lattice temperature simulations.

2. MC algorithm

Numerical implementation of equation (3) involves visiting all the grain boundary sites in the domain during each time-step (MCS), calculating the flipping probability using equation (3) and then executing the flip with the calculated flip probability through a random number generator. The computational algorithm (referred to as algorithm 1 in subsequent text) is shown in figure 1.

The flip probability represented by equation (3) can also be implemented in a different way under special circumstances. Here, all the grain boundary sites are visited during each

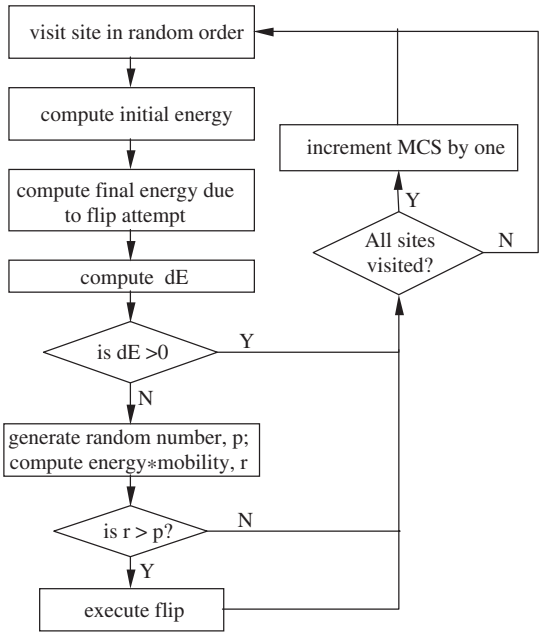

Figure 1. MC simulation algorithm 1 where all boundary sites are visited at each MCS and the probability of flip of a specific boundary site is calculated using $\mu\gamma$ as a kinetic factor.

MCS as in algorithm 1. However, the flip probabilities are calculated by assuming that they are all high-angle boundary sites using the following equation:

$$p(S_i, S_j, \Delta E) = \begin{cases} 1, & \Delta E \leqslant 0, \\ 0, & \Delta E > 0, \end{cases} \tag{4}$$

and scaling the local evolution time for a boundary site, $\Gamma^{\mu\gamma}$, according to

$$\Gamma^{\mu\gamma} = \Gamma \frac{\mu_{\max}\gamma_{\max}}{\mu\gamma}, \tag{5}$$

where Γ is the evolution time per MCS for boundary sites with $\mu = \mu_{\max}$ and $\gamma = \gamma_{\max}$. This approach will be useful for simulating the evolution of different boundary types in one simulation domain provided the different boundary types are physically separated. For example, the shrinking of island grains in one domain with different boundary types could be simulated in this way, recognizing that the total simulation times for the different grains are different. This is possible because the temporal evolution of each island grain is totally independent of the evolution of the other island grains in the domain. However, this approach is not useful when the different boundary types are connected together as in the case of a deformation substructure because it is physically inappropriate to evolve different portions of a connected microstructure to different periods of time. Therefore, this approach will no longer be considered.

An alternate approach to simulating curvature-driven migration using MC technique is proposed in this study where the simulation time of a boundary site (time of visit to a boundary site during simulation) is scaled based on the product of the boundary energy and mobility according to

$$N_{\mathrm{MCS}}^{\mu\gamma} = N_{\mathrm{MCS}} \frac{\mu\gamma}{\mu_{\max}\gamma_{\max}}, \tag{6}$$

where $N_{\mathrm{MCS}}^{\mu\gamma}$ is the simulation time for a given boundary site and N_{MCS} is the simulation time for a site adjacent to the boundary with $\mu = \mu_{\max}$ and $\gamma = \gamma_{\max}$, and the site is flipped using the probability criterion shown in equation (4). It is important to note that in this approach the total physical evolution time for all boundary sites in the domain is the same, although grain boundary sites with different properties are visited for different fractions of the total number of MCS. Therefore, the approach can be applied to real microstructures where the different boundary types are connected together. The computational algorithm for numerically implementing the above approach (referred to as algortithm 2 in subsequent text) is shown in figure 2.

In algorithm 1, $\mu\gamma$ is used as a factor that scales the kinetics of flipping of a boundary site with respect to the kinetics of flipping of the site(s) in the domain that have the maximum value of $\mu\gamma$, namely $\mu_{\max}\gamma_{\max}$. All of the grain boundary sites are visited during an MCS. In algorithm 2 $\mu\gamma$ is used as a time scaling factor that decides right at the beginning of each time step (MCS) the probability of visit to all sites belonging to a boundary type with a given $\mu\gamma$. Therefore, only a fraction of the total boundary sites in the domain is visited during each MCS. It is important to note that in algorithm 2 the grain boundary sites that are visited in a given MCS are all treated as high-angle boundary sites.

The objective of this study is to carry out MC simulations for the shrinking of island grains with different boundary properties using algorithms 1 and 2 and compare the simulation results with theoretical predictions for curvature-driven growth.

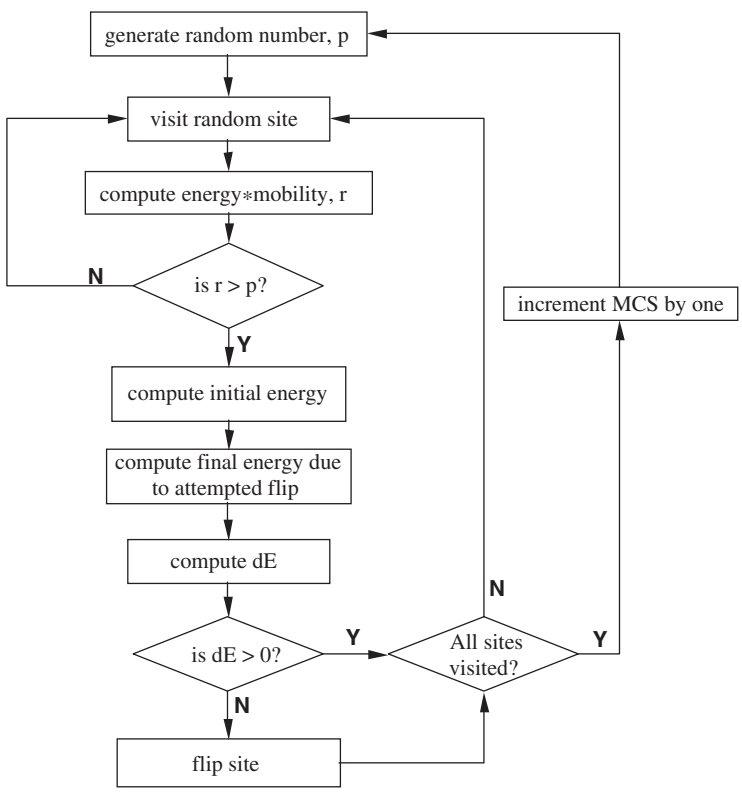

Figure 2. MC simulation algorithm 2 where all boundary sites of a specific type are visited only for a fraction of the simulation time, using $\mu\gamma$ as a time scaling factor.

3. Simulations

Two-dimensional simulations using algorithms 1 and 2 were carried out using a triangular lattice and the neighbourhood for local-energy calculations consisted of the six first-nearest neighbours. The simulation domain consisted of 400 × 200 sites. Initially, two non-overlapping circular grains of diameter 150 lattice units were embedded into the matrix grain. The boundary between one of the circular grains and the matrix was considered to be a high-angle boundary with a relative mobility of 1.0 and relative boundary energy of 1.0. Different grain boundary properties were assigned to the boundary between the second circular grain and the matrix. The simulations yielded the areas of the two circular grains as a function of simulation time. Slopes were obtained for the linear plots of the grain area vs time. From these, the relative slopes were calculated for specific combinations of boundary types and compared with the theoretical values. All simulations were carried out at a zero lattice temperature.

4. Results

Figures 3 and 4 show the variation of the grain area with simulation time for the various boundary types using algorithms 1 and 2, respectively. Both algorithms yield linear plots for the various boundary types used, thus verifying the parabolic shrinking kinetics associated with curvature-driven migration. In both cases, the shrinking rate decreases with decreasing value of $\mu\gamma$ for the boundary, also characteristic of curvature-driven boundary migration. Figure 5 shows the relative slope, $\mu_1\gamma_1/\mu_2\gamma_2$, for the two shrinking grains with $\mu_1\gamma_1 = 1$, and with various input combinations of $\mu_2\gamma_2$ shown in figure 3 for algorithm 1. Figure 6 shows similar data obtained from figure 4 for algorithm 2. Figures 5 and 6 also show the theoretical values of the relative slope for comparison, based on the input values of $\mu_1\gamma_1$ and $\mu_2\gamma_2$. As described previously, $\mu_1\gamma_1$ was kept equal to 1.0 in all the simulations. It is clear from figures 5 and 6 that the use of algorithm 1 leads to a significant deviation between the theoretical and simulated values of the relative slopes while a close agreement is obtained upon using algorithm 2.

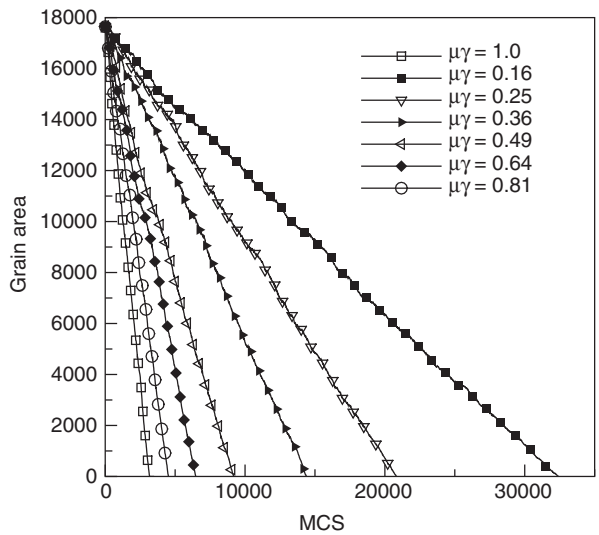

Figure 3. Variation of grain area with simulation time for various grain boundary types using algorithm 1.

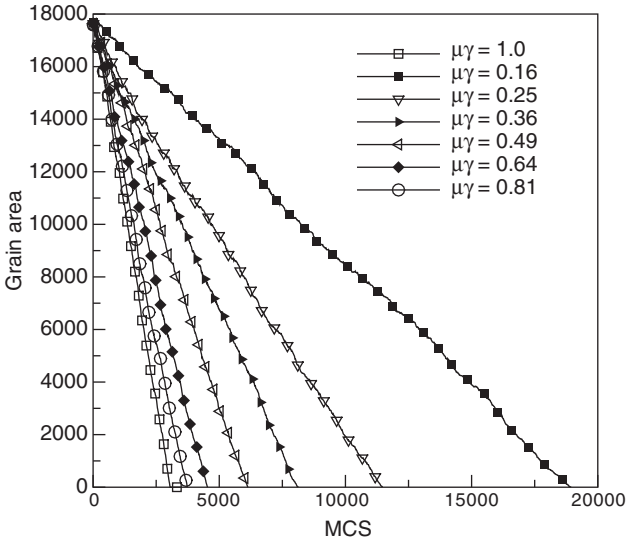

Figure 4. Variation of grain area with simulation time for various grain boundary types using algorithm 2.

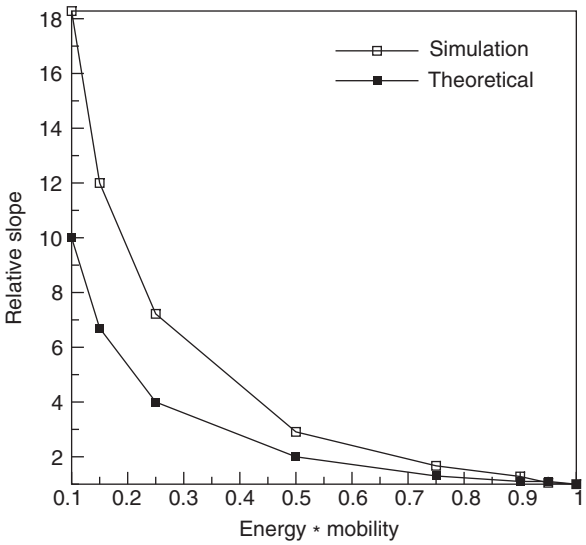

Figure 5. Relative slope, $\mu_1\gamma_1/\mu_2\gamma_2$, as a function of $\mu_2\gamma_2$ with $\mu_1\gamma_1 = 1$ using algorithm 1.

5. Discussion

The main difference between the two algorithms is as follows. In algorithm 1, all the grain boundary sites are visited every time, and the flip probability is scaled by the kinetic factor, $\mu\gamma$, for each site that can potentially flip. However, in algorithm 2, boundary sites corresponding to a specific boundary type are visited only for a fraction of the total simulation time using $\mu\gamma$ as scaling factor for time of visit. Once the visit criterion is met, all the boundary sites are treated alike for flipping purposes as if they are all high angle boundaries with $\mu\gamma = 1.0$.

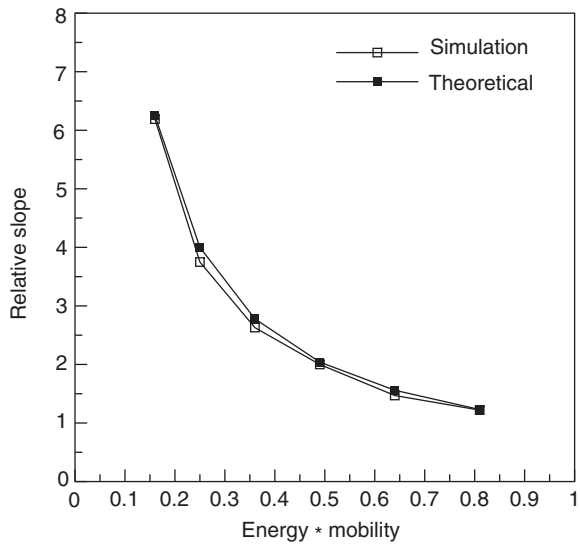

Figure 6. Relative slope, $\mu_1\gamma_1/\mu_2\gamma_2$, as a function of $\mu_2\gamma_2$ with $\mu_1\gamma_1 = 1$ using algorithm 2.

Assume that during the shrinking of a circular grain, there are on an average n_{12} boundary sites in each time step whose flip will result in the reduction of the grain area, and n_{21} sites whose flip will result in the increase of the grain area. Since both algorithms 1 and 2 yield identical results for the shrinking of an island grain with $\mu\gamma = 1.0$, either algorithm can be used to determine n_{12} and n_{21}. Since $n_{12} - n_{21}$ is the net reduction in area per time step, it is the negative slope of the area vs time curves shown in figures 3 and 4. Figure 7 shows the typical result where the cumulative change $\sum(n_{12} - n_{21})$ is plotted as a function of the simulation time. An average value of ~6.0 per MCS is obtained for $n_{12} - n_{21}$.

It can be shown that for $\mu\gamma < 1$ the two algorithms can lead to widely varying results. Consider the situation where the above simulation is continued using algorithm 1 or algorithm 2 after the boundary properties are set to $\mu\gamma = 0.25$. Table 1 shows a rough estimate of the time evolution of n_{12} and n_{21} using the two algorithms for the first four time steps, assuming hypothetical values of $n_{12} = 100$ and $n_{21} = 94$. Note that the use of algorithm 2 results in $\sum(n_{12} - n_{21}) = 6.0$ after 4 MCS, resulting in an average $n_{12} - n_{21}$ per MCS of 1.5. However, algorithm 1 yields $\sum(n_{12} - n_{21}) = 4.2$ after 4 MCS with an average $n_{12} - n_{21}$ per MCS of 1.05. This simplistic analysis shows the mechanistic difference between the two algorithms and explains why the use of algorithm 1 results in a lower rate of reduction of grain area compared to algorithm 2 for a given boundary type.

Figure 8 shows the actual simulation results for the shrinking of a circle with $\mu\gamma = 0.25$ using algorithms 1 and 2. These simulations were started with a geometrically circular grain embedded in a matrix, with boundary properties set to $\mu\gamma = 0.25$. After an initial transient period a steady-state value of $(n_{12} - n_{21})$/MCS is reached. This is approximately 1.5 for algorithm 2 and 0.8 for algorithm 1. Figure 9 shows the simulated temporal evolution of $\sum n_{12}$ and $\sum n_{21}$ using the two algorithms. The difference $\sum(n_{12} - n_{21})$ is seen to increase more rapidly using algorithm 2 than algorithm 1 for the reason described above. It is clear from figure 5 that the shrinking kinetics using algorithm 1 relative to algorithm 2 will be slower the smaller the value of $\mu_2\gamma_2$ relative to $\mu_1\gamma_1/\mu_2\gamma_2$, because the deviation from the theoretical value of the relative slopes increases with decreasing value of $\mu_2\gamma_2$.

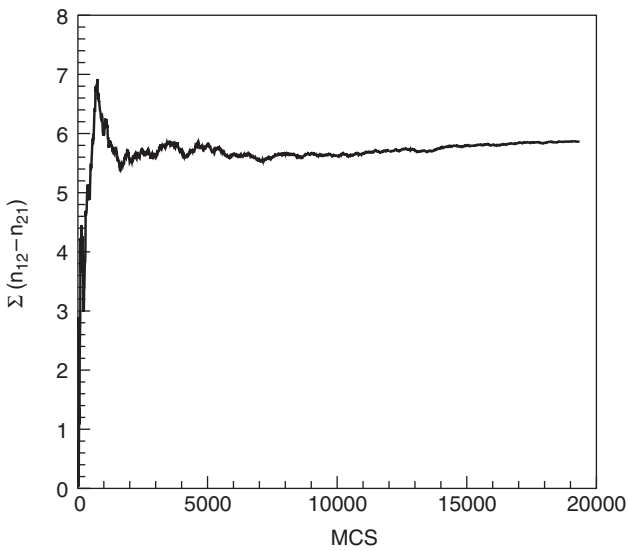

Figure 7. Temporal evolution of $(n_{12} - n_{21})$ per MCS during the shrinking of a circular island grain with $\mu\gamma = 1.0$.

Table 1. Evolution of boundary sites using algorithms 1 and 2.

		Potential n_{12} sites = 100		Potential n_{21} sites = 94		
	MCS	Actual n_{12} flips	Remaining n_{12} sites	Actual n_{21} flips	Remaining n_{21} sites	Actual $\sum(n_{12} - n_{21})$
Algorithm 1	1	25	75	23.5	70.5	1.5
	2	18.8	56.2	17.6	52.9	2.7
	3	14.1	42.1	13.2	39.7	3.6
	4	10.5	31.6	9.9	29.8	4.2
Algorithm 2	1	0	100	0	94	0
	2	0	100	0	94	0
	3	0	100	0	94	0
	4	100	0	94	0	6.0

The MC algorithm has been and is being used widely by many investigators to simulate curvature-driven growth. It is a very popular tool for simulating microstructural evolution in the mesoscale. However, based on published results in the literature, it is not clear whether algorithm 1, which is based on the implementation of equation (2), or algorithm 2, which has been explicitly proposed in this study has been used. The published papers do not provide a detailed explanation of the numerical implementation of the MC technique other than to provide the equations for the switching probabilities for grain boundary sites, such as equation (2). Also, the published results of shrinking circle simulations using the MC technique only demonstrate the fact that the grain area decreases linearly with time. There has been little analysis of the slope of the linear plot of area vs time, and more specifically, the relative slopes of linear plots obtained for the shrinking of island grains with different boundary types. The current simulations prove clearly that the correct values of relative slopes expected for curvature-driven growth are not obtained by using algorithm 1. Such an error has not been reported previously because an analysis of relative slope was not carried out in

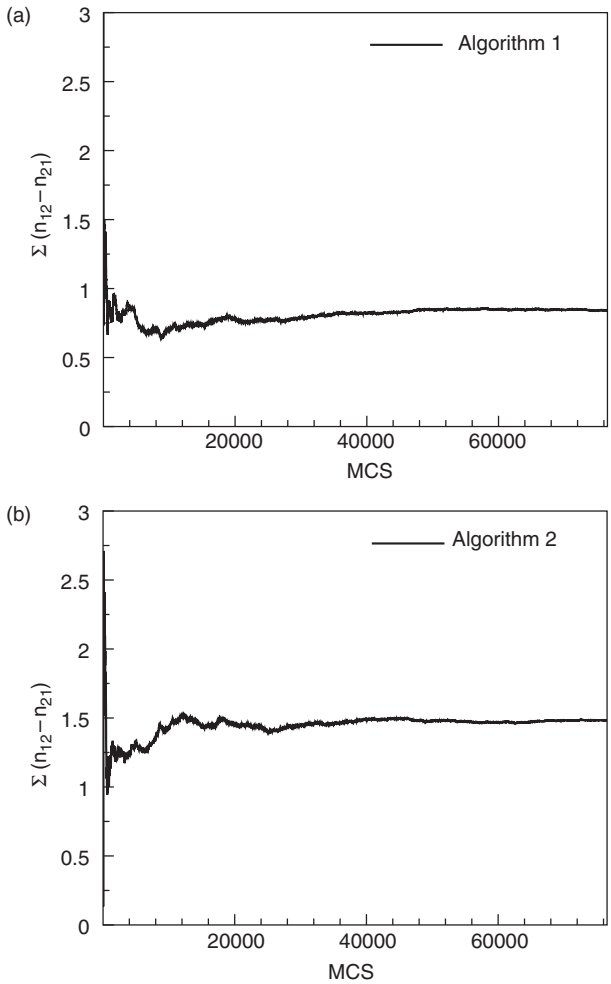

Figure 8. Temporal evolution of $(n_{12} - n_{21})$ per MCS during the shrinking of a circular island grain with $\mu\gamma = 0.25$ using (*a*) algorithm 1 and (*b*) algorithm 2.

previous investigations. It is the opinion of the present authors that algorithm 2 as opposed to algorithm 1 should be used for simulating curvature-driven evolution of grain boundaries when the simulation domain consists of different boundary types.

6. Summary

Two different algorithms for simulating curvature-driven migration by the MC technique have been evaluated. The difference between the two algorithms is quite subtle and it can be easily overlooked in the absence of an analysis of the slope of the linear plot of the area of a shrinking island grain vs simulation time as a function of the grain boundary type. The present simulations show that in order to correctly capture the kinetics of curvature-driven boundary migration it is necessary to scale the simulation time, time of visit to sites adjacent to a given boundary type, according to $\mu\gamma$ rather than visiting all the boundary sites all the time, and flipping them with a probability proportional to $\mu\gamma$.

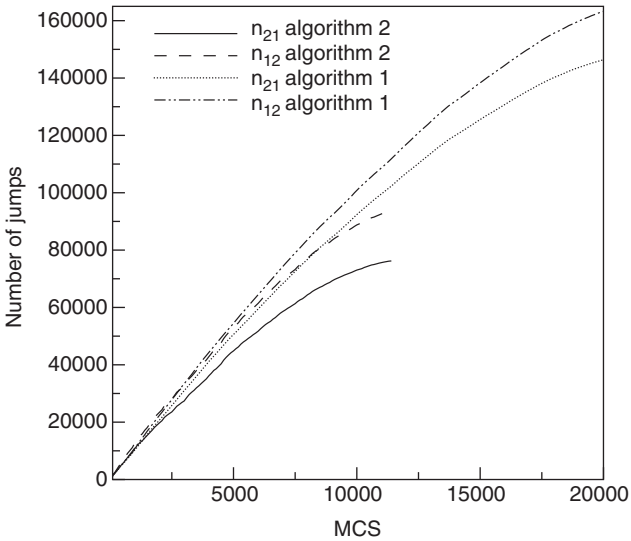

Figure 9. Temporal evolution of the forward and backward jumps during the shrinking of a circle with $\mu\gamma = 0.25$ using algorithms 1 and 2.

Acknowledgments

The authors are grateful to Dr G Sarma, Oak Ridge National Laboratory, for helpful discussions and a critical review of the manuscript. Research sponsored by the Office of Basic Energy Sciences, US Department of Energy, under contract DE-AC05-00OR22725 with UT-Batelle, LLC. The submitted manuscript has been authored by a contractor of the US government under contract No DE-AC05-00OR22725. Accordingly, the US government retains a non-exclusive, royalty-free license to publish or reproduce the published form of this contribution, or allow others to do so, for US government purposes.

References

[1] Srolovitz D J, Anderson M P, Grest G S and Sahni P S 1983 *Scr. Metall.* **17** 241
[2] Chen L Q 1991 *Scr. Metal Mater.* **32** 115
[3] Upmanyu M, Smith R W and Srolovitz D J 1998 *Interface Sci.* **6** 41
[4] Humphreys F J and Hatherly M 1995 *Recrystallization and Related Annealing Phenomena* (Oxford: Pergamon)
[5] Radhakrishnan B, Sarma G, Zacharia T, Kazaryan A and Wang Y 2001 *Microstructure Modeling and Prediction During Thermomechanical Processing* (Indianapolis, IN: The Metallurgical Society) pp 47–56
[6] Rollett A D and Holm E A 1997 *ReX'96 Recrystallization and Annealing Phenomena* (Monterey, CA: MIIS) pp 31–41